

# **Influence of Adsorption on the Measurement of Diffusion Coefficients by Taylor Dispersion**

**G. Madras,<sup>1</sup> B. L. Hamilton,<sup>1</sup> and M. A. Matthews<sup>1,2</sup>**

*Received February 27, 1995*

---

The effect of adsorption on the measurement of diffusion coefficients by the Taylor dispersion technique is investigated by modifying the governing equation to account for reversible, nonequilibrium adsorption. The resulting two-dimensional equations are solved by an explicit finite-difference technique. Experimental data for the acridine-carbon dioxide system indicated that acridine adsorbs on the walls on the tubing and these data were investigated with this model. The influence of various parameters including the number of sites and the rates of adsorption/desorption was investigated by conducting a parametric sensitivity analysis on the model. It was found that adsorption of the solute on the wall of the tubing could produce an error as high as 35% on the measured diffusion coefficient compared to the actual diffusion coefficient. Examination of the influence of each of the parameters will enable future investigators to reduce the effect of adsorption in the measurement of diffusion coefficients by Taylor dispersion.

---

**KEY WORDS:** adsorption; diffusion; supercritical fluid; Taylor dispersion.

## **1. INTRODUCTION**

The knowledge of diffusion coefficients is necessary for understanding any process involving solute transport and also for insight into phenomena such as solute-solvent interactions. Hence, various techniques have been used for the measurement of the diffusion coefficients. These include NMR [1], diaphragm cell [2], and Gouy interference [3]. In recent studies, the

---

<sup>1</sup> Department of Chemical Engineering, University of South Carolina, Columbia, South Carolina 29208, U.S.A.

<sup>2</sup> To whom correspondence should be addressed.

Taylor dispersion (peak-broadening) technique has been extensively used for the measurement of diffusion coefficients [4]. In a typical experiment using this technique, a small pulse of the solute is injected into the solvent flowing in a circular tube, and the concentration at the end of the tubing is obtained. The variance of the concentration profile (response curve) is used to obtain diffusion coefficients. Owing to the relative ease of the experiments and a strong theoretical basis, this technique has been widely used in the measurement of diffusion coefficients of gaseous systems [5], liquid systems [6], and supercritical fluids [7, 8].

Recently, Levelt Sengers et al. [9] have summarized the literature on Taylor dispersion and conducted a thorough investigation of the potential sources of error, especially in the measurement of diffusion coefficients of solutes in supercritical fluids. Clifford and Coleby [10] have also discussed the difficulties involved in measuring diffusion coefficients by Taylor dispersion near the gas-liquid critical point. However, they have not addressed another source of error, namely, the adsorption of the solute on the walls of the tubing. The Taylor dispersion technique assumes that there is no adsorption of the solute. However, this assumption is not always valid; certain solutes, in both liquid and supercritical systems, have been found to be adsorbed on a variety of surfaces like Teflon [11-14], stainless steel [7, 15], and deactivated silica [16, 17]. To account for adsorption, one needs to modify the boundary conditions of the Taylor dispersion model. Therefore, the first objective of the paper is to quantify the error introduced in the diffusion measurements due to the adsorption of the solute on the walls of the tubing. Since the adsorption would be controlled by the number of adsorption sites available, and the rates of adsorption and desorption from the surface of the tubing, these parameters are investigated by conducting a parametric sensitivity analysis on the model.

Another goal of the numerical solution to the Taylor dispersion model with the modified boundary conditions is the evaluation of the magnitude of the adsorption and desorption rate constants. These rate constants are usually determined in packed column chromatography by superimposing an axial dispersion parameter on a radially uniform velocity [18-21]. However, in the case of Taylor dispersion with adsorption in an empty column, the rate constants will be evaluated by solving the two-dimensional Taylor dispersion model in which the radial velocity profile is exactly maintained. This obviates the need for an effective dispersion parameter. Thus, the long-term objective of this study is to expand the utility of the chromatographic peak broadening method for the simultaneous determination of diffusion coefficient as well as adsorption kinetic parameters. This could be accomplished with independent measurements of adsorption and desorption isotherms from a separate experiment.

## 2. MODEL DESCRIPTION

The Taylor dispersion technique was initially developed by Taylor [22, 23] and Aris [24] to study the peak-broadening of a narrow pulse of solute, injected at the entrance of a circular tube. This technique was refined by many investigators including Alizadeh et al. [4] to determine diffusion coefficients of solutes in various fluids.

The continuity equation in terms of molar concentration for cylindrical coordinates assuming laminar flow is given by

$$D_{12} \left[ \frac{\partial^2 C}{\partial r^2} + \frac{1}{r} \frac{\partial C}{\partial r} + \frac{\partial^2 C}{\partial z^2} \right] = -2u \left[ 1 - \left( \frac{r}{R} \right)^2 \right] \frac{\partial C}{\partial z} + \frac{\partial C}{\partial t} \quad (1)$$

where  $D_{12}$  is the molecular diffusion coefficient of solute (1) in a solvent (2) and is assumed to be a constant with respect to concentration. The initial conditions for the above equation ( $t=0$ ) are given by

$$\text{At } z=0: \quad C = C_0 \quad (2a)$$

$$\text{For } z > 0: \quad C = 0 \quad (2b)$$

The boundary conditions ( $t > 0; Z > 0$ ) are given as follows:

$$\left( \frac{\partial C}{\partial r} \right)_{r=0} = 0 \quad (3a)$$

$$\left( \frac{\partial C}{\partial r} \right)_{r=R} = 0 \quad (3b)$$

Further, for an infinitely long tube,

$$\text{For } t > 0 \quad \text{and} \quad z \rightarrow \infty: C = 0 \quad (4)$$

This system of equations can be solved analytically [24] in terms of the radially average mean concentration  $\bar{C}$  to yield

$$\bar{C} = \frac{M}{\pi R^2 (4\pi Kt)^{1/2}} \exp \left( \frac{-(L - \bar{u}t)^2}{4Kt} \right) \quad (5)$$

where  $M$  is the injection mass,  $L$  is the coil length,  $R$  is the radius of the tubing, and  $K$  is the effective Taylor dispersion coefficient [24], given as

$$K = D_{12} + \frac{R^2 \bar{u}^2}{48D_{12}} \quad (6)$$

A key assumption in the model is that the solute does not adsorb on the walls of the tubing and is given by the boundary condition, Eq. (3b). Golay [25] has derived equations that describe the solute diffusion when the rate of adsorption of the solute on the walls of the tubing is fast (i.e., equilibrium adsorption is achieved). In this case the real diffusion coefficient can be related to the apparent value

$$D_{12} = D_{\text{app}} \frac{(1 + 6k + 11k^2)}{(1 + k)}, \quad \text{with} \quad k = \frac{t_a - t_0}{t_0} \quad (7)$$

where  $k$  is the capacity factor, and  $t_1$  and  $t_0$  are the retention times of the adsorbed and unadsorbed solute, respectively. However, as pointed out by Loh et al. [11], this equation does not fully account for the solute adsorption encountered with their experimental data. Further, one needs to develop equations which would be valid for nonequilibrium reversible adsorption of the solute on the walls. Equation (3b), the wall boundary condition, needs to be modified to include this effect. For this purpose, we consider the radial flux of solute at the wall to be

$$N_1 = -D_{12} \left[ \frac{\partial C}{\partial r} \right]_{r=R} + y_1(N_1 + N_2) \quad (8)$$

where  $y_1$  is the solute mole fraction in the mobile phase, evaluated at the tube wall ( $r = R$ ). For small values of  $y_1$ , Eq. (3b) becomes

$$\left[ \frac{\partial C}{\partial r} \right]_{r=R} = -\frac{N_1}{D_{12}} \quad (9)$$

Since the concentration of the solute in the fluid is very low, and the maximum coverage cannot exceed monolayer, the Langmuir isotherm was chosen for the evaluation of the flux of the solute

$$\begin{aligned} N_1 &= r_{\text{ads}} - r_{\text{des}} \\ r_{\text{ads}} &= k_a C(1 - \Phi) \\ r_{\text{des}} &= k_d \Phi \\ \frac{\partial \Phi}{\partial t} &= \frac{r_{\text{ads}} - r_{\text{des}}}{S} \end{aligned} \quad (10)$$

where  $\Phi$  is the fractional surface coverage and  $S$  is the total number of active sites per unit surface area.  $k_a$  and  $k_d$  are the adsorption and desorption rate constants. The equation is rewritten with a dimensionless concen-

tration  $C^*$ , given by normalizing the concentration by the saturation concentration ( $C_0$ )

$$\frac{\partial \Phi}{\partial t} = -N_s [k'_a \phi - k'_d C^*(1 - \phi)] \quad (11)$$

where  $N_s$  can be considered as a flux scaled by the surface area and has the units of inverse time,  $k'_a$  and  $k'_d$  are dimensionless and are the adsorption rate constants scaled to the diffusion rate and are given by

$$N_s = \frac{C_0 D_{12}}{RS}; \quad k'_d = \frac{Rk_d}{C_0 D_{12}}; \quad k'_a = \frac{Rk_a}{D_{12}} \quad (12)$$

Boddington and Clifford [26] have developed analytical solutions for the dispersion of material where adsorption, desorption, and irreversible reaction occur. The method of moments was used to obtain solutions, and in the case where reaction did not occur, their solutions were equivalent to the open-tubular chromatography analysis of Golay [25]. Under the conditions investigated by Boddington and Clifford, all predicted response curves were Gaussian, and the effect of adsorption and desorption was to increase the rate and extent of dispersion of the original pulse input. Experimental evidence [11–17], as well as our computational results (to be presented), shows a distinct non-Gaussian shape is discernible. It may be that neglect of certain terms which decay exponentially is the cause of this discrepancy. Reconciliation of the analytical solution and the numerical solution should be sought.

### 3. EXPERIMENT

Alizadeh et al. [4] have provided a complete review of the theory of the Taylor dispersion. They have also provided criteria in terms of mean velocity of the solute peak,  $\bar{u}$ , in the dispersion tube under which the experiments are to be conducted. Adherence to these criteria ensures that the effects of secondary flow are negligible, the flow is laminar, and experimental errors due to mechanical features of the injection and detection devices are minimized. The experimental data used in this study were taken from Smith et al. [27] and Hamilton [16]. The maximum standard deviation of the experimental data was less than 4%. The experimental response curve for phenanthrene was Gaussian and the diffusion coefficients were directly extracted from the response curve. However, with the same experimental apparatus, the response of the acridine-carbon dioxide

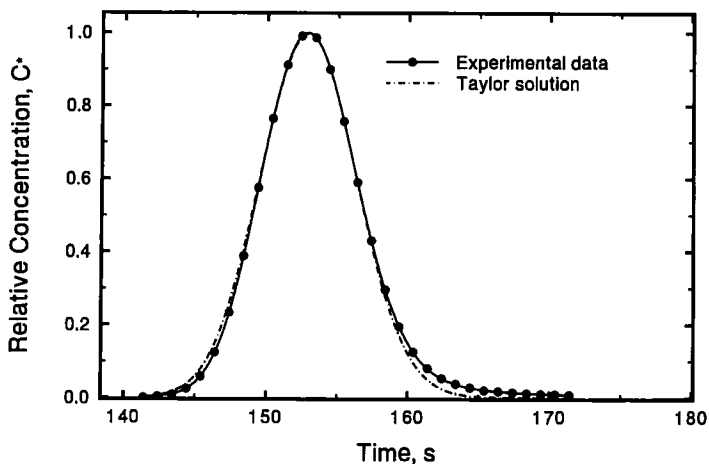


Fig. 1. Non-Gaussian response curve of the acridine-carbon dioxide system.

system is non-Gaussian due to the adsorption of acridine on the surface of deactivated silica, as shown in Fig. 1. The non-Gaussian response of the system is due only to adsorption, since all the criteria proposed by Alizadeh et al. [14] have been met, and the response of phenanthrene-carbon dioxide system under the same experimental conditions and apparatus is Gaussian. Hence, the response curve should not be analyzed using the usual technique to extract the diffusion coefficients.

#### 4. NUMERICAL MODELING

Equation (a) is solved with the above boundary conditions with an explicit finite difference scheme. For each approximation, a second-order finite-difference approximation was used. Because of the peculiarity of the initial condition (pulse input), wherein the concentration is discontinuous initially, numerical dispersion occurs, resulting in severe numerical errors. The problem of flow with steep density gradients was investigated by Boris and Book [28]. They developed an algorithm which treats these steep density (or concentration) gradients and minimizes the induced numerical error. This algorithm, called the Flux-Corrected Transport (FCT) algorithm, has been previously used to model the Taylor dispersion by Mayock et al. [29]. He concluded that the algorithm successfully limits the numerical error encountered due to the pulse injection. The algorithm consists of two parts, the transport stage and the antidiffusion stage. In the transport stage, a numerical dispersion term is added to the transport equation.

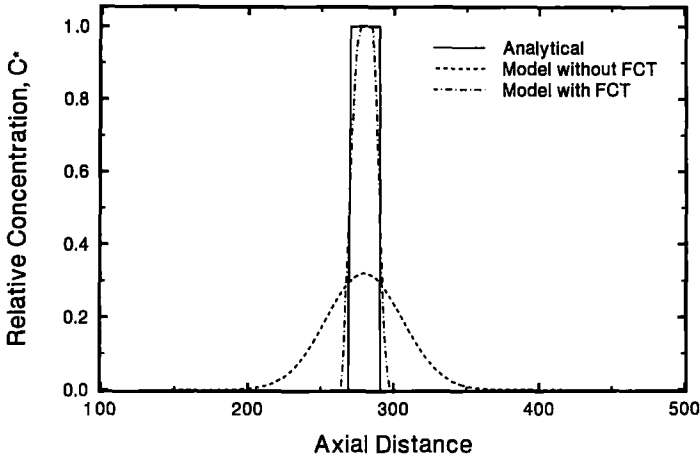


Fig. 2. Plug flow modeling of a pulse (need of FCT).

In the anti-diffusion stage, the numerical dispersion term is corrected. Figure 2 depicts the need for this algorithm. Consider the hypothetical case of injecting a square of solute in a conduit wherein the mobile phase moves in a plug flow and there is neither diffusion nor adsorption. The result should be the original narrow square pulse, displaced some distance down the conduit. If this is modeled using finite differences alone, numerical dispersion occurs creating a dispersed and apparent Gaussian response. When the FCT algorithm is employed to this hypothetical case, the true solution is obtained. The reason for the effectiveness of the algorithm is that it is mass conservative, meaning that any correction applied to a single node is counteracted by adding the opposite correction to the appropriate adjacent node. An integral part of the FCT algorithm involves finding an estimate for the numerical dispersion coefficient. The problem is finding an optimum value of the numerical dispersion coefficient such that the numerical error is a minimum. In this model, the numerical dispersion coefficient  $K'$ , was calculated using an equation given by Book et al. [30],

$$e = \frac{2u(1 - (r^*)^2) dt}{dz}; \quad K' = \frac{3e(1 - e/2)}{4(1 + e)^2} \tag{13}$$

**4.1. Modeling of the Injection and Detector Output**

In this model, it is assumed that the simulation starts at time 0, immediately following the injection. Consequently, it is useful to think of

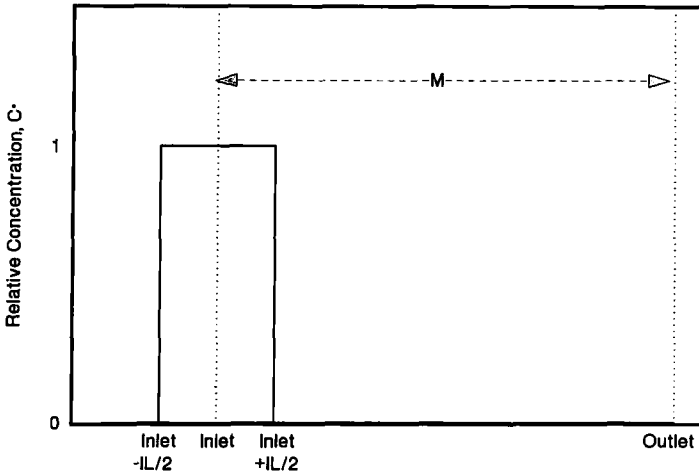


Fig. 3. Modeling of the injection.

the diffusion tube to be divided into  $M$  longitudinal or axial elements. Initially the concentration in all elements is zero, except for the region containing the pulse injection, where  $C^*$  is equal to unity. This is illustrated in Fig. 3. The boundary conditions, given by Eqs. (2a) and (2b), will be modified as

$$\text{At } t = 0, \quad \text{where } \frac{-IL}{2} \leq z \leq \frac{IL}{2}; \quad C^* = 1.0 \quad (14a)$$

$$\text{At } t = 0, \quad \text{where } z < \frac{-IL}{2} \quad \text{and} \quad z > \frac{IL}{2}; \quad C^* = 0.0 \quad (14b)$$

Next, one needs to deal with the output of data. The numerical model gives concentration at each axial and radial element, but in a physical experiment one records the radially averaged concentration with respect to time. This is done physically by placing a detector at the end of the diffusion tube and recording the concentration signal as function of time. To simulate the physical detector with the model, the concentration is averaged at an axial position which corresponds to the end of the tube. For each iteration, the average concentration is recorded with the cumulative time. This gives a direct simulation to the physical experiment, and hence the data from the model can be compared directly to the experiment.



#### 4.2. Verification of the Model

The first test for the numerical scheme was to assume a hypothetical case by imposing a velocity profile which is a constant across the radial cross section and setting the molecular diffusion terms to zero. As discussed earlier, and shown in Fig. 2, the model with the FCT algorithm is able to predict the analytical solution to a fair degree of accuracy.

The next step was to verify the ability of the model to predict a Gaussian response by simulating an actual experiment, wherein the solute does not adsorb on the tube. For this purpose, the experimental data of diffusion of phenathrene in supercritical carbon dioxide at 308 K and 27.7 MPa were used. The parameters  $R$  and  $L$  were physically measured and are 0.11 mm and 1.549 m, respectively. The parameters  $D_{12}$  and mean velocity  $\bar{u}$  were taken from the analytical Taylor solution and were 8.168 and  $0.00855 \times \text{m} \cdot \text{s}^{-1}$ , respectively. To simulate the experiment, the above parameters were used in the numerical model. The spatial increments were fixed as  $dr = 0.0333$ ,  $dz = 0.005163$  m, and the time step was fixed to be 0.00075 s. The injection volume was calculated from the experiment and was between 0.1 and  $0.5 \mu\text{l}$ . Since the axial spatial increment is known, the dimensionless injection length corresponding to an injected volume of  $0.2 \mu\text{l}$  was 10 elements. Figure 4 shows the model output with the data and the Taylor dispersion coefficient. The figure shows that the model is able accurately to predict an experimental response and the error between the diffusion coefficient calculated from the model response curve and the true (input) coefficient is negligible. Hence, one can conclude that the model is

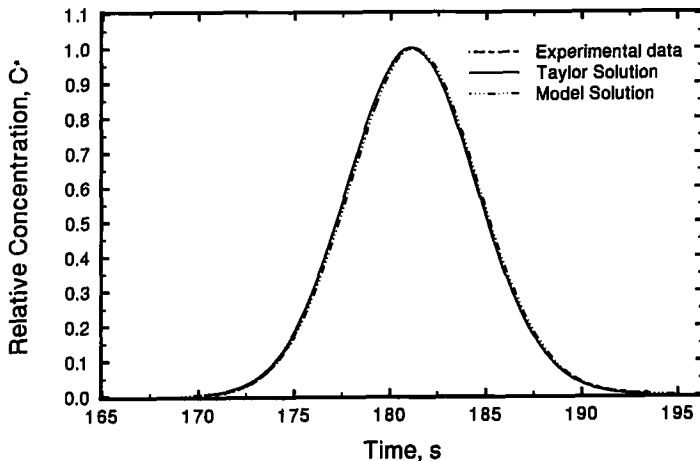


Fig. 4. Prediction of a Gaussian response by the model.

accurate and is successful in predicting both the hypothetical case and the Taylor dispersion experiment.

### 4.3. Numerical Error Analysis

The final step was to conduct an error analysis to identify the sources of numerical error and optimize the spatial and the time increments to reduce the computation time. The effect of radial increment was investigated by dividing the dimensionless tube radius into 15, 30, and 60 elements. Increasing the number of radial elements over 30 does not cause a significant decrease in numerical error to warrant the increase in computational time.

A similar study on the axial elements was performed with the tube divided into 1000, 2000, and 3000 axial increments. The injection width was fixed at 10 axial elements for 3000 axial increments and was adjusted proportionally depending on the number of the axial increments. The numerical error is minimized for the case wherein the tube is divided into 3000 axial points.

The time increment used in the numerical solution was also studied. The model was found to be unstable for time increments above 0.001 s. Simulations were run using time increments of 0.00025, 0.0005, and 0.00075 s and the error from the model was investigated as a function of time increment and it was found that decreasing the time increment below 0.00075 s has no substantial impact on the numerical error. Because the model was found to be stable, and was capable of simulating a variety of cases successfully, the model was used to simulate various cases of solute adsorption.

## 5. RESULTS AND DISCUSSION

The non-Gaussian response of the acridine-carbon dioxide system was modeled with the modified equations of the Taylor dispersion model accounting for adsorption. To model the equations, one requires an estimate of the number of sites available on the fused silica and the rates of adsorption/desorption. Since the adsorption of acridine on silica may be due to the hydroxyl groups present on the surface of deactivated silica, the number of hydroxyl sites on fused silica reported by Wright et al. [31] was used as an initial guess of the total number of available sites for adsorption,  $S = 3.49 \times 10^{-7} \text{ mol.m}^{-2}$ , which corresponds to  $N_s$  of  $6000 \text{ s}^{-1}$ . With the value of  $N_s$  at  $60,000 \text{ s}^{-1}$  (small value of the number of sites,  $S$ ), the fractional coverage at any given time will be complete, say 0.99. This would

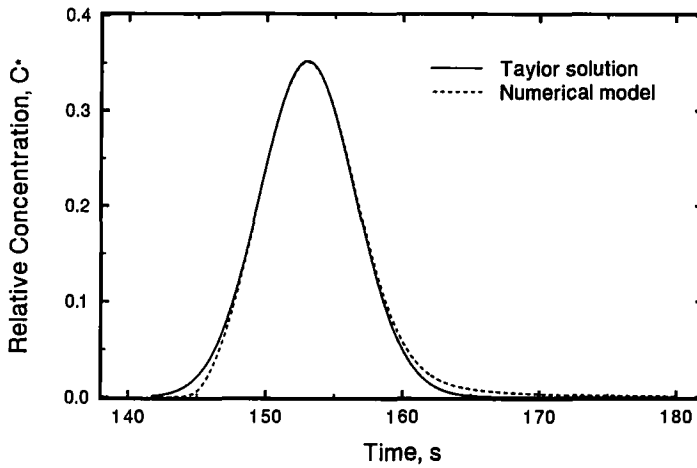


Fig. 5. Prediction of the non-Gaussian response curve.

yield the fraction available for adsorption to be in the order of 0.01, implying that the desorption rate constant must be approximately 100 times smaller than the adsorption rate constant for the rates to be equal. Using these values of rates of adsorption and rates of desorption, the model is able to predict the non-Gaussian response well, as shown in Fig. 5. This suggests that there are not enough active sites for chromatographic peak retention to occur, yet there are enough active sites available to retain part of the peak, hence making it tail.

Two limiting checks on the model can be carried out at this stage, by decreasing the number of the sites to zero, and increasing the number of sites to infinity. In the limit of zero sites ( $N_s \rightarrow \text{large} = 4 \times 10^6$ ), the peak should show no tailing. The model was run under these conditions, and the results are shown in Fig. 6. It can be seen that the model predicted no tailing, as expected. The other limiting case is to allow for unlimited number of adsorption sites ( $N_s \rightarrow \text{small} = 0.1$ ) which would correspond to the simulation of chromatography. There should be no change in the peak shape, i.e. the response should be Gaussian, but the peak retention time should be greatly increased due to solute retention. The results of this simulation are shown in Fig. 7. It can be seen that the peak is still Gaussian, however, its retention time has increased from  $\sim 180$  to  $\sim 215$  s, as expected. This verifies that the model is capable of predicting various hypothetical cases.

The final step is to use the model to simulate the response curve for various values of adsorption sites, and rates of adsorption and desorption.

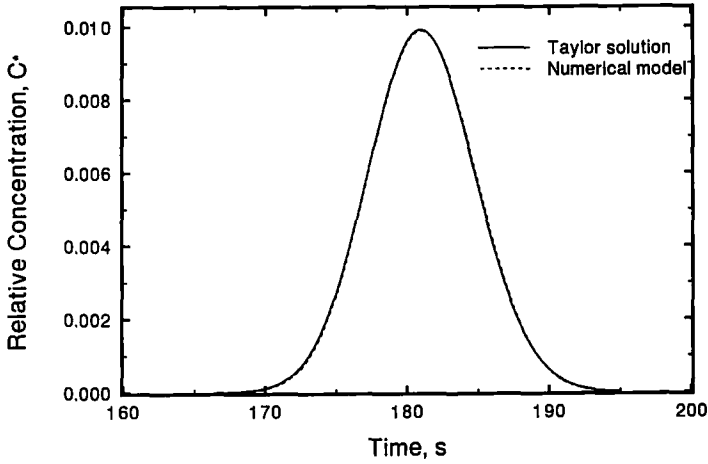


Fig. 6. Hypothetical case of sites  $\rightarrow$  zero.

The effect of the number of sites on silica on the response curve of Taylor dispersion was studied by varying  $N_s$  by an order of magnitude, as shown in Fig. 8. Both the extent of tailing and the retention time increase with decreasing  $N_s$ . Thus, the shape of the peak is sensitive to the number of sites available for adsorption. The effect of the rates of adsorption and desorption on the response curves is dependent upon the number of sites available for adsorption. For example, at a small value of  $N_s$ , the effect of

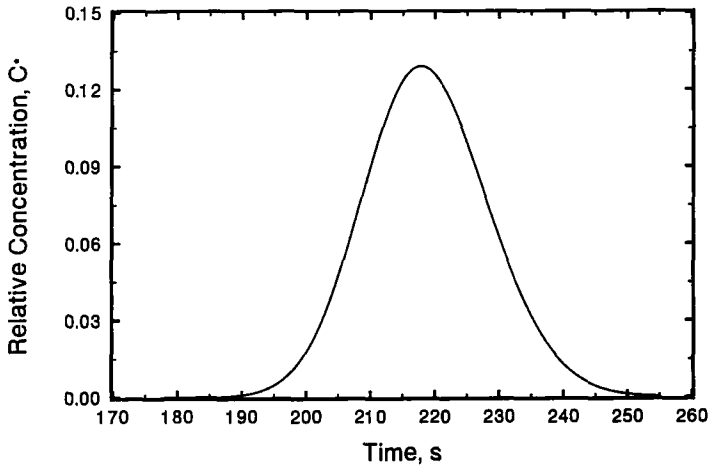


Fig. 7. Hypothetical case of sites  $\rightarrow$  infinity.

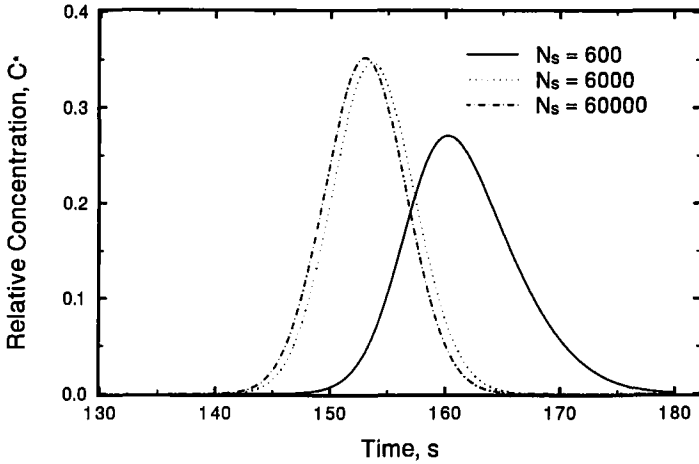


Fig. 8. Effect of  $N_s$  on the Taylor dispersion model.

the rates on the response curve is significant, as shown in Fig. 9. However, as  $N_s$  increases, the effect of these rates become less important in influencing the shape of the response curve. This can be seen from Figs. 10 and 11. At a large value of  $N_s$ , the influence of the adsorption/desorption nearly disappears, as shown in Fig. 11. In each of these cases, the apparent diffusion coefficients are extracted from these hypothetical cases and compared to the actual diffusion coefficient. The results in Figs. 6 and 8–11 are quantified in Table I, which shows the effect of adsorption parameters,  $k_a$ ,  $k_d$ ,

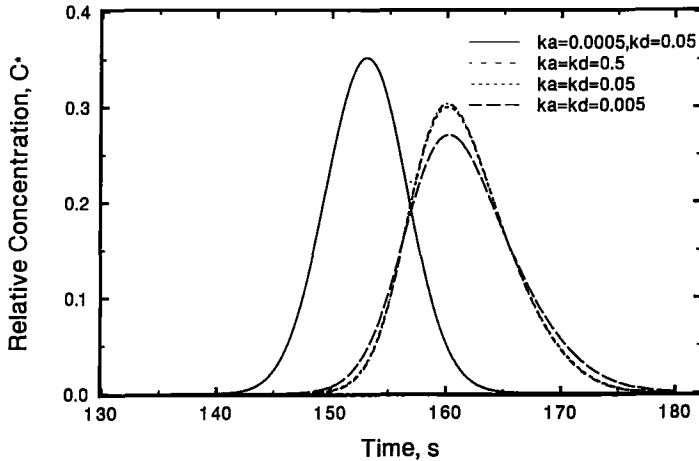


Fig. 9. Effect of  $k_a$ ,  $k_d$  on the Taylor dispersion model at  $N_s = 600 \text{ s}^{-1}$ .

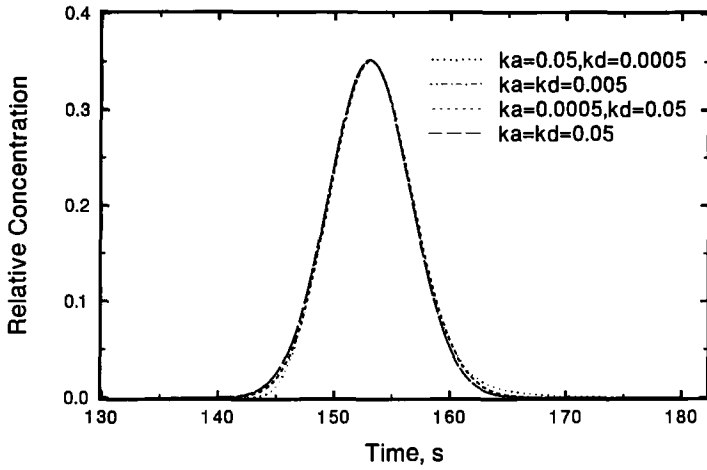


Fig. 10. Effect of  $k_a, k_d$  on the Taylor dispersion model at  $N_s = 60000 \text{ s}^{-1}$ .

and  $N_s$  on the "observed" diffusion coefficient. That is, the response curves predicted by the model were fit to the Taylor (Gaussian) solution and the observed diffusion coefficient was obtained from that fit. As seen from Table I, the error in the observed diffusion coefficient can be significant and proves that the observed diffusion coefficients are significantly different than the actual diffusion coefficient when the solute adsorbs on the walls of the tubing.

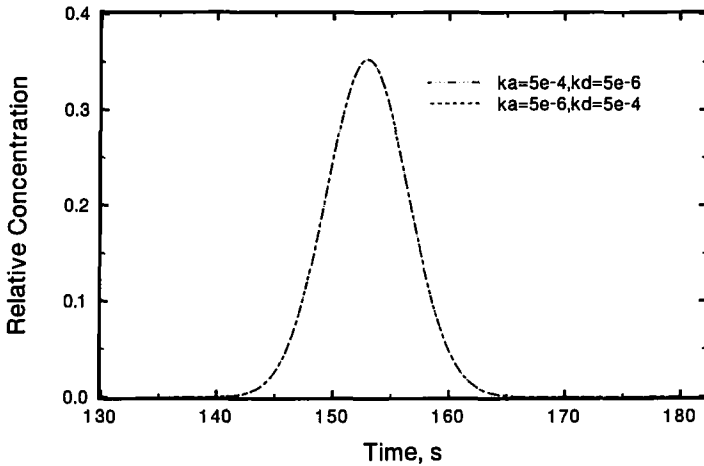


Fig. 11. Effect of  $k_a, k_d$  on the Taylor dispersion model at  $N_s = 4 \times 10^6 \text{ s}^{-1}$ .

Table I. Effect of Various Parameters on Observed Diffusivities:

$$D_{\text{actual}} = 6.696 \times 10^{-9} \text{ m}^2 \cdot \text{s}^{-1}$$

Variable parameter	Observed $D_{12}$ ( $\times 10^{-9} \text{ m}^2 \cdot \text{s}^{-1}$ )	% error $= (D_{\text{actual}} - D_{\text{observed}})/D_{\text{actual}}$
Case 1: $k_a = k_d = 0.005$		
$N_s = 600 \text{ s}^{-1}$	4.36	34.88
$N_s = 6000 \text{ s}^{-1}$	6.56	2.03
$N_s = 60,000 \text{ s}^{-1}$	6.69	0.01
Case 2: $N_s = 600 \text{ s}^{-1}$		
$k_a = 0.0005, k_d = 0.05$	6.54	2.32
$k_a = k_d = 0.5$	5.33	20.4
$k_a = k_d = 0.05$	5.23	21.89
$k_a = k_d = 0.005$	4.36	34.88
Case 3: $N_s = 60000 \text{ s}^{-1}$		
$k_a = 0.05, k_d = 0.0005$	6.69	0
$k_a = k_d = 0.005$	6.69	0.02
$k_a = 0.005, k_d = 0.05$	6.53	2.39
$k_a = k_d = 0.05$	6.69	0.02
Case 4: $N_s = 4 \times 10^6 \text{ s}^{-1}$		
$k_a = 5 \times 10^{-4}, k_d = 5 \times 10^{-6}$	6.53	2.48
$k_a = 5 \times 10^{-6}, k_d = 5 \times 10^{-4}$	6.69	0.08

## 6. SUMMARY

When care is taken to eliminate experimental artifacts from the Taylor dispersion experiment, the presence of a skewed response curve is strong evidence of dynamic, nonequilibrium adsorption between the solute and the surface of the diffusion tube. The numerical model described herein semi-quantitatively reproduces experimental response curves. The parameters in this model are the concentration of surface sites, the adsorption and desorption kinetic constants, and the diffusion coefficient. The parametric studies show that a variety of known chromatographic phenomena can be predicted, from classical Taylor dispersion to ideal open tubular chromatography. At intermediate values of surface concentration and kinetic parameters, where the effects of adsorption produce skewed response curves, the error between actual and predicted diffusion coefficient is as high as 35% (Table I).

Because a wide variety of materials (stainless steel, teflon, fused silica) normally used in Taylor dispersion apparatus have shown evidence of adsorption, the accuracy of this method may be compromised. Previous analyses (e.g., Ref. 4) of the experimental procedure for Taylor dispersion have focused on mechanical aspects of the apparatus, while adsorption is clearly a chemistry-dependent phenomena. Experimentalists should thus consider performing the Taylor dispersion experiment with different materials for the diffusion tube, if adsorption effects are anticipated. The present study provides some numerical estimates of the potential errors. However, precise quantitative corrections for dispersion may require independent measurement of certain of the parameters, e.g., concentration of active surface sites.

## REFERENCES

1. P. Stilbs, *Progr. NMR Spectrosc.* **19**:1 (1987).
2. A. J. Easteal, *Can. J. Chem.* **68**:1611 (1990).
3. L. Paduano, R. Sartori, V. Vitagliano, and L. Costantino, *J. Solut. Chem.* **19**:31 (1990).
4. A. Alizadeh, C. A. Nieto De Castro, and W. A. Wakeham, *Int. J. Thermophys.* **1**:243 (1980).
5. J. C. Giddings and S. L. Seager, *J. Chem. Phys.* **33**:1579 (1960).
6. K. C. Pratt and W. A. Wakeham, *Proc. R. Soc. London* **336**:393 (1974).
7. R. Feist and G. M. Schneider, *Sep. Sci. Technol.* **17**:261 (1982).
8. P. A. Wells, R. P. Chaplin, and N. R. Foster, *J. Supercrit. Fluids* **3**:8 (1990).
9. J. M. H. Levelt Sengers, U. K. Deiters, and G. M. Schneider, *Int. J. Thermophys.* **14**:893 (1993).
10. A. A. Clifford and S. E. Coleby, *Proc. Roy. Soc. Lond.* **A433**:63 (1991).
11. W. Loh, C. A. Tonegutti, and P. L. O. Volpe, *J. Chem. Soc. Faraday Trans.* **89**:113 (1993).
12. F. Galembeck, *J. Polym. Sci. Polym. Lett.* **16**:1315 (1978).
13. J. Yao and G. Strauss, *Langmuir* **7**:2353 (1991).
14. I. C. S. F. Jardim, M. Sartoratto, P. R. Salida, C. Archundia, and K. E. Collins, *Appl. Radiat. Isot.* **40**:643 (1989).
15. M. Orejuela, M.S. thesis (Texas A&M University, College Station, 1994).
16. B. L. Hamilton, M. S. thesis (University of Wyoming, 1992).
17. V. M. Shenai, B. L. Hamilton, and M. A. Mathews, *In Supercritical Fluid Engineering Science—Fundamentals and Applications*, J. F. Brennecke and E. Kiran, eds. (American Chemical Society, Washington, DC, 1993).
18. C. Erkey and A. Akgerman, *AIChE J.* **36**:1715 (1990).
19. J. J. Shim and K. P. Johnston, *AIChE J.* **37**:607 (1991).
20. N. Wakao, S. Kagueli, and J. M. Smith, *Ind. Eng. Chem. Res.* **19**:363 (1980).
21. H. W. Haynes, *Catal. Rev. Sci. Eng.* **30**:563 (1988).
22. G. Taylor, *Proc. R. Soc. London* **219**:186 (1953).
23. G. Taylor, *Proc. R. Soc. London* **225**:473 (1954).
24. R. Aris, *Proc. R. Soc. London* **235**:67 (1956).
25. M. J. E. Golay, in *Gas Chromatography*, D. H. Desty; ed. (Butterworth, London, 1959).



26. T. Boddington and A. A. Clifford, *Proc. Roy. Soc. London A.* **179**: (1983).
27. S. A. Smith, V. M. Shenai, and M. A. Matthews, *J. Supercrit. Fluids* **3**:175 (1990).
28. J. P. Boris and D. L. Book, *J. Comp. Phys.* **11**:38 (1973).
29. K. P. Mayock, J. M. Tarbell, and J. L. Duda, *Sep. Sci. Tech.* **15**:1285 (1980).
30. D. L. Book, J. P. Boris, and K. Hain, *J. Comp. Phys.* **18**:248 (1975).
31. B. W. Right, M. L. Lee, and G. M. Booth, *Chromatographia* **15**:584 (1982).